Calcium- and BTB domain protein-modulated PINOID protein kinase directs polar auxin transport

Robert-Boisivon, H.S.

Chapter 5

A BTB domain protein interacts with the protein kinase PINOID to fine tune its activity

Hélène Robert, Marcelo K. Zago, René Benjamins[1], Yang Xiong[2], Carlos Galván-Ampudia, Ab Quint, Niels Wattel, Douwe Doevendans, Fang Huang, Remko Offringa

[1] Current address: Molecular Genetics Group, Department of Biology, Utrecht University, Padualaan 8, 3584 CH Utrecht, The Netherlands.

[2] Current address: College of Life Sciences, Peking University, Beijing 100871, China

Abstract

Polar transport of auxin directs plant development by producing dynamic gradients through the concerted action of asymmetrically localized PIN-FORMED (PIN) auxin efflux carriers. The PINOID (PID) serine/threonine protein kinase determines the direction of auxin transport by regulating the polar subcellular targeting of PIN proteins. A yeast two-hybrid screen using PID as bait identified *Arabidopsis thaliana* BTB and TAZ domain protein1 (BT1) as PID BINDING PROTEIN2 (PBP2). In Arabidopsis, *BT1/PBP2* belongs to a small gene family comprising five members, encoding proteins with the same land plant-specific domain structure: an N-terminal BTB domain, a TAZ domain and a C-terminal Calmodulin binding domain. At least four of the five BT proteins interact with PID through their BTB domain, and *in vitro* phosphorylation assays indicate that BT1 is not a target for phosphorylation by PID, but that BT1 binding reduces its kinase activity. BT1 localizes in the nucleus and the cytoplasm, and upon co-expression with PID, BT1 is found at the plasma membrane whereas PID becomes partially nuclear. Overexpression of BT1 leads to a reduction of *PID* gain-of-function seedling phenotypes and enhanced *pid* loss-of-function embryo phenotypes. Furthermore, *bt* loss-of-function rescues seedling phenotypes and enhances adult plant phenotypes of *35Spro:PID* plants. Together these data indicate that on the one hand BT1 functions as a repressor of PID kinase activity, and that on the other hand recruitment of PID by the BT-orchestrated protein complex is a crucial aspect of PID signaling. We present evidence that the BT1 scaffold protein is possibly involved in feed back control between PID-directed auxin transport and KNOX-BEL controlled internode patterning in the inflorescence.

Introduction

The phytohormone auxin plays a crucial function in plant developmental processes such as embryogenesis, phyllotaxis and root meristem maintenance (Sabatini et al., 1999, Reinhardt et al., 2003, Benková et al., 2003). Characteristic for auxin action is its polar transport, which generates gradients and maxima that are instrumental in directing cell division, -elongation and -differentiation (Tanaka et al., 2006). Auxin transport can be chemically inhibited resulting in inflorescence meristems that lose the capacity to produce leaves and flowers and therefore form pin-like structures (Okada et al., 1991). The Arabidopsis *pin-formed1* (Okada et al., 1991) and the *pinoid* (Bennett et al., 1995) loss-of-function mutants phenocopy plants that have been treated with polar auxin transport inhibitors. The *PIN-FORMED1* (*PIN1*) gene is part of a family of eight genes in Arabidopsis that encodes major transporter membrane proteins characterized by two groups of five conserved transmembrane domains (Paponov et al., 2005). These PIN proteins were shown to be the

rate limiting factor in auxin efflux (Petrášek et al., 2006) and to determine the direction of polar auxin transport through their asymmetric subcellular localization (Wisniewska et al., 2006). The *PINOID* (*PID*) gene encodes a plant specific protein serine/threonine kinase (Christensen et al., 2000) that has been implied as a regulator of polar auxin transport (Benjamins et al., 2001), and was shown to induce the subcellular targeting of PIN proteins to the apical (shoot apex facing) plasma membrane (Friml et al., 2004). Recent evidence that PID was able to phosphorylate the PIN proteins allowed to identify the mechanism of PID-dependent PIN targeting (Michniewicz et al., 2007). In order to clarify this pathway, we used PID as bait in a yeast two-hybrid screen to identify PID BINDING PROTEINs (PBPs). Two of these PBPs, TOUCH3 (TCH3) and PBP1, are calcium-binding proteins that regulate PID kinase activity in *in vitro* phosphorylation assays (Benjamins et al., 2003), suggesting the involvement of calcium in regulating and directing auxin-mediated plant development.

Here we analyze the functional interaction of PID with PBP2, a BTB (Broad-Complex, Tramtrack, Bric-à-Brac) domain protein that was previously identified as a potato calmodulin interactor, and was named BT1 after BTB and TAZ domain protein1 (Du and Poovaiah, 2004). BTB domain proteins are known to act as scaffold- or linker-proteins that organize protein complexes (Albagli et al., 1995). The Arabidopsis genome encodes eighty BTB domain proteins that can be grouped in ten subfamilies (Gingerich et al., 2005). Most of the BTB proteins contain a second protein domain that specifies their function (Motchoulski and Liscum, 1999, Sakai et al., 2000, Wang et al., 2004, Weber et al., 2005, Dieterle et al., 2005). Besides the N-terminal BTB domain, BT1 contains two additional protein-protein interaction domains: a TAZ domain (Transcriptional Adaptor Zinc finger) (Ponting et al., 1996) and a C-terminal calmodulin binding domain (Du and Poovaiah, 2004). Our data demonstrate that PID interacts with the BTB domain containing part of BT1, and that BT1 is not a phosphorylation target of PID but a repressor of its kinase activity. Overexpression of BT1 reduces PID overexpression phenotypes and enhances *pid* loss-of-function phenotypes. Using GFP-tagged proteins, we show that BT1 co-localizes with PID at the plasma membrane, and also causes PID to localize to the nucleus. This nuclear localization of PID is only observed in the presence of BT1, and suggests a new function for PID signaling in the nucleus. Interestingly, phenotypes obtained by meristem-specific ectopic expression of the BTB domain of BT1 suggest a link between the KNOX-BEL transcription factors and PID-regulated polar auxin transport during internode patterning in the inflorescence. Apart from BT1, also other members of the BT protein family were found to interact with PID, and a multiple *bt* knock-out rescued *PID* gain-of-function seedling phenotypes, suggesting that despite their function as multifunctional scaffolds, their role as regulator of PID is conserved for all BT proteins.

Results

PINOID interacts with BT proteins through their BTB domain

Two Arabidopsis yeast two-hybrid cDNA libraries were screened for proteins that interact with the PID protein serine/threonine kinase (Benjamins, 2004). One of the identified PID partners was BT1/PBP2. BT1 contains an N-terminal BTB domain, which is well-known to mediate both homo- and hetero-dimerization of proteins (Bardwell and Treisman, 1994, Figueroa et al., 2005, Weber et al., 2005), and two other protein-protein interaction domains: a TAZ domain that also mediates protein-protein interactions (Ponting et al., 1996) and a C-terminal domain that was found to interact with a potato calmodulin CaM6 (Du and Poovaiah, 2004) (Figure 1A). To test which domain binds to PID, GST-tagged full length BT1, or the GST-tagged BTB or TAZ domains alone (Figure 1A) were incubated *in vitro* with crude extracts from *E. coli* cell expressing His-tagged PID. Western blot analysis using anti-His antibodies showed that PID efficiently binds the BTB domain, whereas the TAZ domain only pulls down background levels of the kinase (Figure 1B).

BT1 is part of a small protein family comprising five members in Arabidopsis that not only share the BT1 domain structure, but also interact with the same proteins. The five Arabidopsis BT proteins have been shown to bind the potato CaM6, and BT1, BT2 and BT4 were found to interact with bromodomain transcription factors (Du and Poovaiah, 2004). To test the possibility that PID also binds other BT family members, *in vitro* pull-down assays were performed using His-tagged BT1, -BT2, -BT4 and -BT5. All four proteins were efficiently pulled down from a crude *E. coli* extract by the GST-tagged PID, but not by the GST tag alone (Figure 1C). Although we were not able to test His-BT3, our results suggest that PID is a conserved interaction partner for all five Arabidopsis BT proteins. Genetic and expression analyses of the *BT* family already indicated that there is functional redundancy between the *BT* genes (Chapter 4, this thesis), and our results suggest that the BT proteins also act redundantly in the PID pathway.

BT1 is a likely regulator of PID kinase activity

PID is an auto-activated protein serine/threonine kinase that can auto- and trans-phosphorylate in *in vitro* reactions (Figure 1D, lane 1) (Christensen et al., 2000, Benjamins et al., 2003), thus we tested whether BT1 is a PID phospho-target *in vitro*. No phosphorylation of BT1 was observed, but, interestingly, the presence of BT1 in the reaction mixture resulted in a significant reduction of the PID kinase activity, as indicated by the reduced levels of PID auto-phosphorylation and of the phosphorylation of the general protein kinase substrate Myelin Basic Protein (MBP) (Figure 1D). These results suggest that BT1 has a negative effect on both auto- and trans-phosphorylation activity of PID and imply that BT1 is not a target of PID phosphorylation, but that instead it functions as a negative regulator of PID activity.

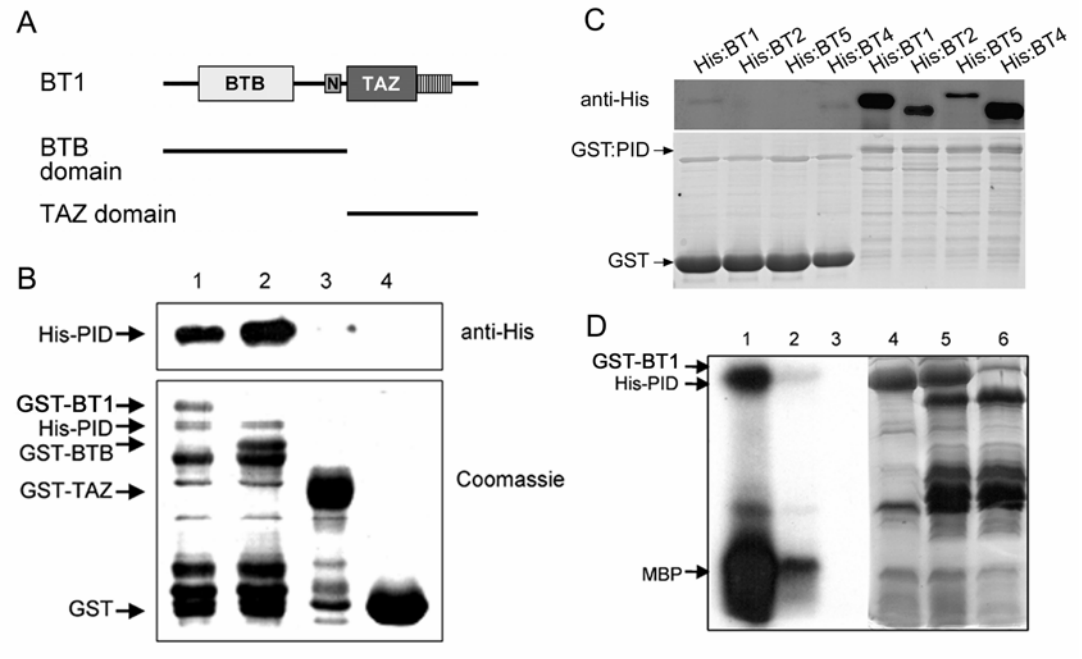

Figure 1. Binding of PINOID to the BTB domain of BT1 represses its kinase activity *in vitro.*
(A) Schematic representation of BT1 (365 aa) and the two deletion versions comprising either the BTB or the TAZ domains. The N-box and the striped box indicate the positions of respectively a nuclear localization signal (aa 193-203) and a putative calmodulin binding site (Du and Poovaiah, 2004).
(B) Western-blot analysis (top panel) with anti-His antibodies detects His-tagged PID after pull-down with GST:BT1 (lane 1) or the GST-tagged BTB domain (lane 2), but not with the GST-tagged TAZ domain (lane 3) or GST alone (lane 4), from the soluble fraction of *E. coli* protein extracts. The bottom panel shows the Coomassie stained gel of the pull-down reactions, with the positions of the different proteins indicated.
(C) Western blot with the anti-His antibody (top panel) showing specific pull-down of His-tagged BT1, -BT2, -BT5 and -BT4 by GST-tagged PID (right), and only background levels when GST is used in the pull-down assay (left). The bottom panel represents a Coomassie stained gel of the same experiment showing the presence of the GST and the GST-tagged PID.
(D) Autoradiograph (lanes 1, 2 and 3) and Coomassie stained gel (lanes 4, 5 and 6) of a phosphorylation assay containing PID and MBP (lanes 1 and 4), PID, BT1 and MBP (lanes 2 and 5), or BT1 and MBP (lanes 3 and 6).

BT1 *expression overlaps with that of* PINOID

For PID and BT1 to interact *in planta,* it is crucial that their spatio-temporal expression patterns overlap. To investigate this, Northern blot analysis was performed and the results were compared with the available Genevestigator micro-array data (Zimmermann et al., 2004) and the previously published *PID* expression pattern (Christensen et al., 2000, Benjamins et al., 2001). *PID* expression is most abundant in roots, young developing flowers and siliques, and it is expressed at relatively low levels in seedling and plant shoots (Figure 2A). In these tissues, PID is expressed in the young vascular tissues and around

organ primordia (both in root and shoot) (Benjamins et al, 2001). *BT1* mRNA is particularly abundant in seedling shoots, but can also be detected in seedling roots, and in stems and flower buds (Figure 2B). Furthermore, the expression of both *PID* and *BT1* is auxin inducible (Figure 2C). These data indicate that *PID* and *BT1* expression patterns partially overlap, which corroborates a possible *in vivo* interaction between the two proteins.

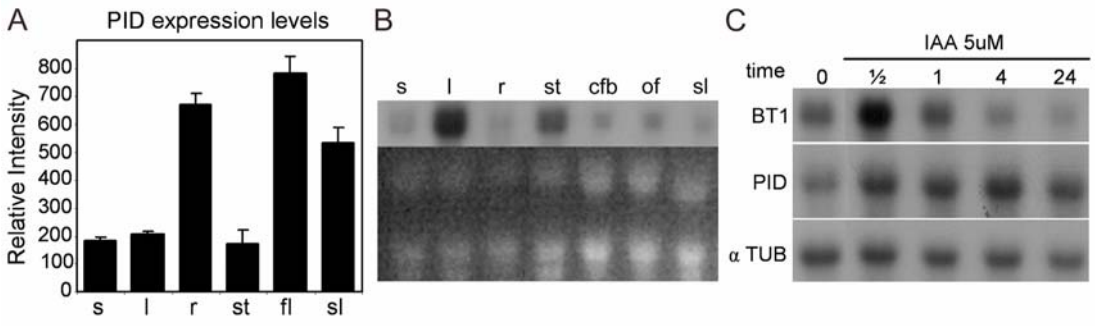

Figure 2. The auxin responsive *BT1* gene is co-expressed with *PID.*
(A) The Genevestigator micro-array data show that *PID* expression is high in roots (r), flowers (fl) and siliques (sl), and lower in seedlings (s), leaves (l) and stems (st).
(B) Northern blot analysis showing the expression of *BT1* mRNA in wild-type Arabidopsis Columbia tissues. Leaf (l) and root (r) tissues are from 2-week old seedlings (s). Stems (st), flower buds (cfb), opened flowers (of) and siliques (sl) are from 6-week old plants.
(C) Northern blot showing that *BT1* (upper panel) and *PID* (middle panel) expression is induced in 8-day old seedlings as soon as 30 min after auxin treatment. The expression of *αTubulin* (lower panel) is used as loading control.

PID and BT1 co-localize at the plasma membrane and in the nucleus

Previous experiments indicated that PID is a plasma membrane-associated protein (Lee and Cho, 2006), whereas BT1 is predominantly nuclear localized in *35Spro:BT1:GFP* transfected protoplasts or in *35Spro:BT1:GFP* plant lines (Chapter 4, this thesis). This raised the question where PID and BT1 meet in the cell to form a complex. Closer inspection of *35Spro:PID:GFP* transfected protoplasts revealed however, that only 38 % of the protoplasts showed purely plasma membrane localization of PID:GFP (Figure 3A, n = 122), and that in 62 % PID:GFP is both at plasma membrane and in the cytosol (Figure 3B). This corresponds to more recent observations using a *PIDpro:PID:VENUS* Arabidopsis line (Michniewicz et al., 2007), and indicates that PID and BT1 can meet in the cytosol.

Co-transfection of Arabidopsis protoplasts with *35Spro:PID:CFP* and *35Spro:BT1:YFP* indeed showed the expected overlap in localization in the cytosol.

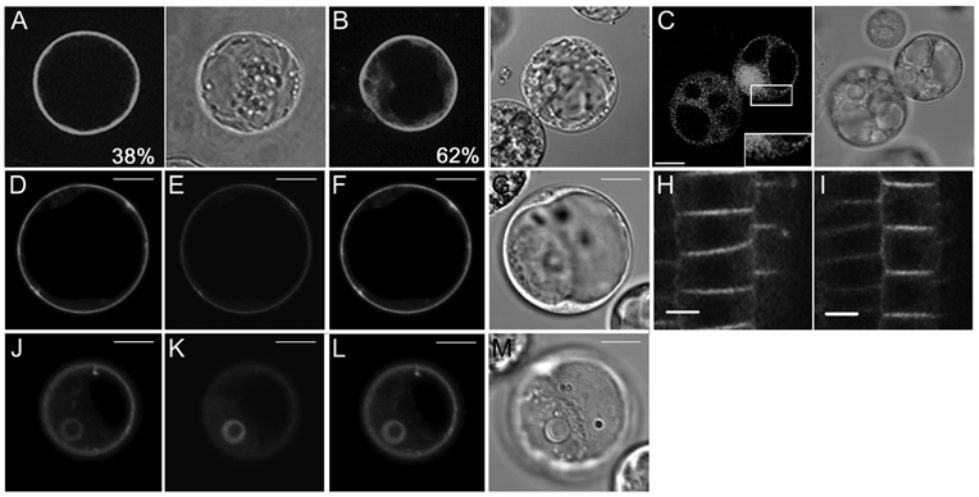

Figure 3. BT1 and PID co-localize at the plasma membrane and in the nucleus in Arabidopsis protoplasts.
(A-C) Confocal images (left) and the corresponding transmission light images (right) of representative Arabidopsis protoplasts transfected with *35Spro:GFP:PID* (A, B) or *35Spro:BT1:YFP* (C). In 38 % of the cells GFP:PID localizes at the plasma membrane (A), whereas 62 % of the cells show both cytosolic and plasma membrane localization (B). BT1:YFP localizes in the nucleus and the cytosol (C), but no clear signal is observed at the plasma membrane (detail).
(D-G) and (J-K) Different confocal sections of an Arabidopsis protoplast co-transfected with *35Spro:PID:CFP* and *35Spro:BT1:YFP*. PID:CFP shows plasma membrane (D), cytosolic (D, J) and nuclear (J) localization, whereas BT1:YFP, beside its normal cytosolic and nuclear localization (K), now localizes at the plasma membrane (E). Merged (F, L) and transmitted light (G, M) images are shown.
(H-I) A confocal microscopy section through the root meristem shows the subcellular localization of PID in epidermal cells in *PIDpro:PID:VENUS* (H) and in *PIDpro:PID:VENUS 35Spro:BT1-1* (I).
Scale bars are 10 µm.

Interestingly, however, in the co-transfected cells a clear signal was observed for BT1:YFP at the plasma membrane (Figure 3E), whereas PID:CFP could now be detected in thenucleus (Figure 3J). Control transfections with single constructs showed plasma membrane and cytosolic localization for PID:CFP, and nuclear and cytosolic localization for BT1:YFP (data not shown). Not only do these results provide important *in vivo* evidence for the interaction between PID and BT1, but they also indicate that a portion of BT1 is recruited to the plasma membrane through its interaction with PID, whereas PID is imported to the nucleus upon BT1 interaction (Figures 3D-F and 3J-L). The nuclear localization of the BT1-PID complex suggests that one of the functions of BT1 in the PID signaling pathway is to regulate the subcellular localization of PID, and also uncovers a new role for PID signaling in the nucleus. We used *35Spro:BT1:GFP* and *PIDpro:PID:VENUS* plants to find *in planta* evidence for the BT1-mediated nuclear import of PID. However, BT1:GFP localization and instability was not affected in a *PID*-overexpression background (data not shown), neither did *BT1* overexpression significantly

alter the baso-apical plasma membrane localization of PID:VENUS in root epidermal cells of seedlings (Figures 3H and 3I). The difference between the observations in protoplasts and in plants may be explained by the fact that BT1 in plants, due to its instability (see Chapter 4, this thesis), is not sufficiently abundant to visualize the recruitment of PID or BT1 to respectively the nucleus and the plasma membrane.

Overexpression of* BT1 *enhances* pid-14 *phenotypes and inhibits* 35Spro:PID *root collapse

To obtain more *in vivo* conformation on the possible role of BT1 as negative regulator of PID activity, we generated *35Spro:BT1* overexpression lines and selected two lines showing significantly increased *BT1* transcript levels for further analysis (Figure 4A). As neither of them showed mutant phenotypes, we examined the effect of *BT1* overexpression on the intermediately strong *pid-14* allele. About 40 % of the *pid-14* mutant embryos developed three instead of two cotyledons (Bennett et al., 1995), and in the *BT1* overexpression background the penetrance of the tricotyledon phenotype was significantly increased up to 58 % (Figures 4B and 4F). In addition, seedlings with more severe cotyledon phenotypes were observed, such as no-cotyledons (1 %, Figure 4C), monocotyledons (2 %, Figure 4D) and even tetracotyledons (1 % only for *35Spro:BT1-2 pid-14*, Figure 4E), phenotypes that were never found among progeny of the *pid-14* mutant line (Figure 4F). These severe phenotypes are observed in some strong *pid* alleles (Bennett et al., 1995), indicating that *BT1* overexpression enhances the mutant phenotypes of the *pid-14* allele during embryo development, which fits with a role of BT1 as negative regulator of PID. At adult plant stage, however, no phenotypes additional to the typical *pid* inflorescence were observed.

To further support the previous results, we also crossed the selected overexpression lines *35Spro:BT1-1* and *-2* with the *35Spro:PID-21* overexpression line. *PID* overexpression leads to the absence of auxin accumulation at the root meristem due to a polarity switch in the subcellular localization of PIN auxin efflux carriers (Friml et al., 2004). This results in agravitropic root growth and in the differentiation of root meristem initials, leading to the collapse of the main root meristem (Benjamins et al., 2001). *35Spro:PID-21*-induced root meristem collapse is observed in 17 % of the seedlings at 3.5 days after germination (dag) and in 91 % of the seedlings at 5.5 dag (Figure 4G and Benjamins et al, 2001). Overexpression of *BT1* resulted in a significant reduction of the *35Spro:PID-21* induced root collapse between 3.5 (3 % and 7 % for *PID-21 BT1-1* and *-2* respectively) and 5.5 dag (71 % and 80 % for *PID-21 BT1-1* and *-2*, respectively) (Figure 4G). The level of *PID* overexpression in *35Spro:PID-21 35Spro:BT1-2* did not significantly differ from that in the parental *35Spro:PID-21* line (Figure 4A), but in *35Spro:PID-21 35Spro:BT1-1* we can not completely exclude that reduced root collapse is

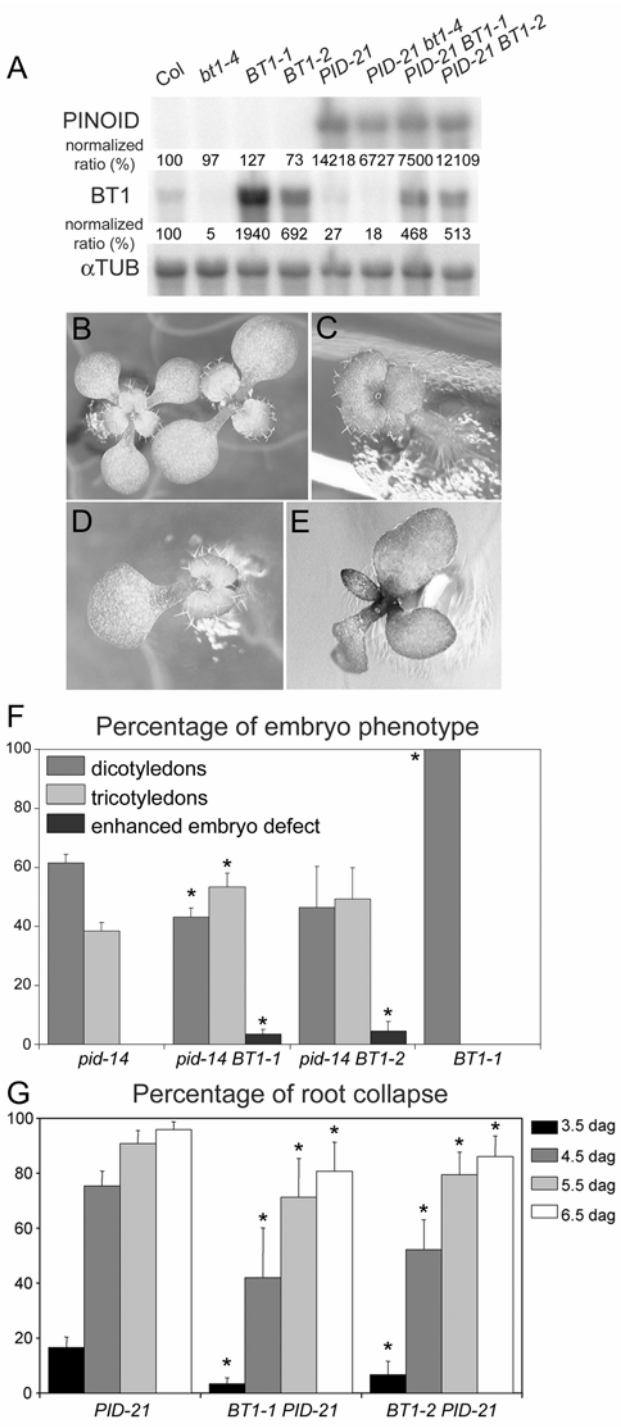

Figure 4. Overexpression of *BT1* enhances *pid-14* embryo phenotypes and inhibits *35Spro:PID-21* root meristem collapse.

(A) Northern blot analysis showing *PINOID* (top), *BT1* (middle) and *αTubulin* (bottom) expression in seedlings of the Col wild-type, *bt1-4*, the *35Spro:BT1* overexpression lines -1 and -2, *35Spro:PID-21* and in seedlings of the crosses *35Spro:PID-21 bt1-4*, *35Spro:PID-21 35Spro:BT1-1* and *35Spro:PID-21 35Spro:BT1-2*. The expression levels were quantified using ImageQuant, corrected for loading differences using *αTubulin* as a reference and normalized to the expression level in wild type.

(B) Segregation of cotyledon phenotypes observed in the *pid-14* mutant line, with the tricotyledon phenotype (left) indicative for seedlings homozygous for the *pid-14* allele.

(C-E) The enhanced cotyledon phenotypes observed in the *pid-14 35Spro:BT1* line range from no cotyledon (C), monocotyledon (D) and tetracotyledon (E) seedlings.

(F) Graph showing the proportion of tri- and di-cotyledons seedlings and seedlings with enhanced embryo phenotype (no-, mono- or tetracotyledons) in *pid-14* (n = 290, 424, 298), *pid-14 35Spro:BT1-1* (n = 372, 658, 367), *pid-14 35Spro:BT1-2* (n = 302, 688, 408) and *35Spro:BT1-1* (n = 191, 193). Stars (*) indicated that the values are significantly higher compared to *pid-14* (Student's t-test, $p < 0.05$).

(G) Graph showing the percentage of root collapse at 3.5, 4.5, 5.5 and 6.5 days after germination (dag) in *35Spro:PID-21* (n = 199, 186, 275), *35Spro:PID-21 35SproBT1-1* (n = 233, 321, 344), *35Spro:PID-21 35Spro:BT1-2* (n = 214, 315, 348). For each time point the values of the *35Spro:PID-21 35Spro:BT1* lines were significantly lower than those of *35Spro:PID-21* (Stars (*), Student's t-test, $p < 0.01$).

due to reduced *PID* expression levels. Together these results corroborate our previous conclusion that BT1 is a negative regulator of PID activity. Similar to the single overexpression lines, no striking phenotype could be observed in *35Spro:PID-21 35Spro:BT1* lines at adult plant stage.

BT1 ***overexpression does not change PIN1 and PIN2 localization in the root***

Previously, we have shown that PID is required for the correct asymmetric subcellular localization of PIN proteins and that above-threshold levels of PID expression causes the apicalization of the PIN proteins (Friml et al., 2004, Michniewicz et al., 2007). To investigate whether the observed negative effect of BT1 on PID activity results in changes in PIN polar targeting, we immunolocalized PIN1 and PIN2 in wild type, *35Spro:PID-21*, *35Spro:BT1-1* and *35Spro:PID-21 35Spro:BT1-1* seedlings. As expected, in wild type roots, PIN1 localized at the basal (root tip facing) membrane in endodermis and stele cells (Figure 5A), whereas PIN2 localized basally in the epidermis and apically (shoot apex facing) in the cortex (Figure 5B). In *35Spro:PID-21* seedlings roots, PIN1 and PIN2 localized to the apical plasma membrane in the cells where they are expressed. No significant changes in PIN1 or PIN2 localization were observed in root tips of *35Spro:BT1-1* or *35Spro:PID-21 35Spro:BT1-1* seedlings as compared to wild type or *35Spro:PID-21*, respectively (Figure 5). These observations indicate that *BT1* overexpression does not reverse the effect of PID overexpression on the subcellular PIN1 and PIN2 localization in root tips, and suggest that BT1 is involved in fine-tuning rather than completely inhibiting PID kinase activity.

PID-BT interaction is necessary for proper PID signaling

The inability of *BT* overexpression to induce changes in PIN localization indicates that BT is not merely a negative regulator of PID kinase activity. BT proteins may rather be involved in fine-tuning PID action, either by down-regulating its activity, or by offering another subset of phospho-substrates through the recruitment of PID to a specific domain of the cell (such as the nucleus). To further test this possibility and since our analysis of the Arabidopsis BT family in Chapter 4 of this thesis indicated that there is considerable functional redundancy among the *BT* genes, and we show here that at least four of the five Arabidopsis BT proteins interact with PID, we introduced the *PID* overexpression locus of line *35Spro:PID-21* in *bt* quintuple loss-of-function mutant background. *35Spro:PID-21 bt1 bt2/+ bt3/+ bt4 bt5* plants are bushy and have even shorter siliques than *bt1 bt2/+ bt3/+ bt4 bt5*, whereas siliques length of *35Spro:PID-21* plants does not significantly differ from wild type siliques (Table 1). Since quintuple homozygous seedlings in *35Spro:PID-21* background could not be obtained, we conclude that *PID* overexpression does not rescue the gametophytic lethality of the *bt* quintuple mutant (Chapter 4, this thesis). The seedling phenotype observed in *35Spro:PID-21*, collapse of the main root meristem and root

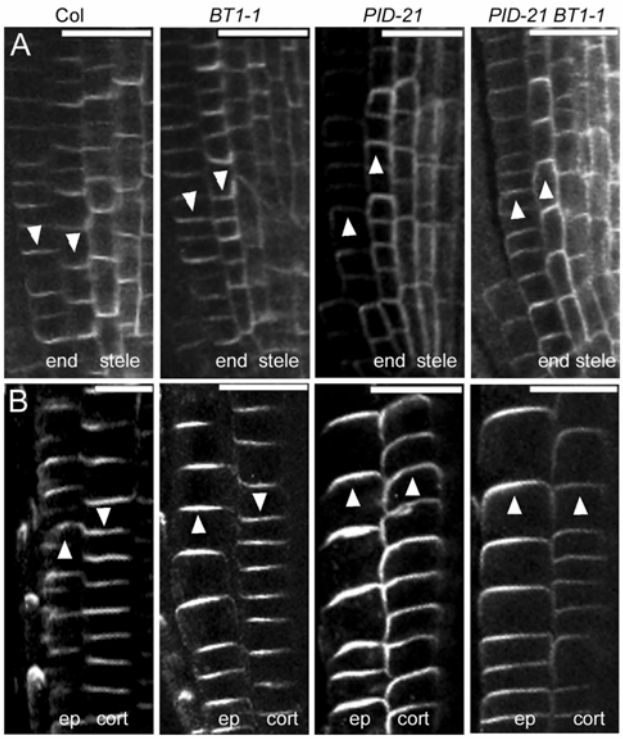

Figure 5. PIN1 and PIN2 polar targeting is not significantly changed by *BT1* overexpression.
Immunolocalization of PIN1 (A) and PIN2 (B) in Arabidopsis Columbia wild type, *35Spro:BT1-1*, *35Spro:PID-21* and *35Spro:PID-21 35Spro:BT1-1*.
(A) PIN1 is expressed in the endodermis (end) and stele of the root tip, where it is localized at the basal (root tip facing) plasma membrane in wild type and *35Spro:BT1-1* root tips, whereas apical (shoot apex facing) PIN1 localization can be observed in these cell layers in both *35Spro:PID-21* and *35Spro:PID-21 35Spro:BT1-1* root tips.
(B) PIN2 is expressed in the cortex (cort) and in the epidermis (ep) where it shows respectively basal and apical localization in wild type and *35Spro:BT1-1* roots. In *35Spro:PID-21* and *35Spro:PID-21 35Spro:BT1-1* root tips, PIN2 localizes apically in both cell layers.
Scale Bars are 50 μM.

Table 1. *bt* loss-of-function leads to reduced silique length.

	silique length (mm)*	s. d.	n
Col	15	1.3	5
bt1 bt2/+ bt3/+ bt4 bt5	8.7[*]	1.6	7
35Spro:PID-21	14.4	1	5
35Spro:PID-21 bt1 bt2/+ bt3/+ bt4 bt5	5.3[*†#]	0.6	6

[*] Significantly different from Col wild type (Student's t-test, $p < 0.01$)
[†] Significantly different from *35Spro:PID-21* (Student's t-test, $p < 0.01$)
[#] Significantly different from *bt1 bt2/+ bt3/+ bt4 bt5* (Student's t-test, $p < 0.01$)

agravitropism, is absent in *35Spro:PID-21 bt1 bt2/+ bt3/+ bt4 bt5* seedlings. These observations indicate that the two characteristics of *PID* overexpression in seedlings were rescued by the (nearly) absence of the BT function in *bt1 bt2/+ bt3/+ bt4 bt5*. Although we can not exclude that *PID* overexpression levels are reduced in the quintuple *bt* mutant background, the fact that the presence of the *35Spro:PID-21* construct does have a strong effect on the development of the quintuple mutant at the adult plant stage indicates that the overexpression construct is still actively transcribed. Based on these results we conclude

that BT proteins are not merely negative regulators of PID activity, but that the PID-BT complex is an essential signaling component.

Meristem-specific BTB domain expression leads to flower and axillary branching defects

For *PID*, the *35S* promoter is not sufficiently strong during embryogenesis or inflorescence development to induce clear phenotypic defects at these stages. Only when *PID* expression was placed under control of the cell division-specific *RPS5A* promoter (Weijers et al., 2001, Weijers et al., 2003), strong defects related to auxin transport were observed in these tissues (Friml et al., 2004). Since *35S* promoter-controlled overexpression of *BT1* or its BTB domain alone did not provide mutant phenotypes, we decided to test their overexpression using the *RPS5A* promoter. *RPS5Apro>>BT1* plants showed no clear developmental defects, and also *RPS5Apro>>BTB* seedlings were normal upon germination. In 7- to 8-week old *RPS5Apro>>BTB* plants, however, significant defects in floral development and axillary branching could be observed. Flower initiation at the primary inflorescence meristem terminated prematurely, and the flowers that were formed were aberrant and did not set seed (Figure 6A). Correlating with this, 7-week old *RPS5Apro>>BTB* plants showed reduced apical dominance and developed significantly more secondary inflorescences (3.5 to 4.75 [for 3 independent transformants, n = 8] compared to 2.1 for Col wild-type [n = 8]). In comparison, *RPS5Apro>>PID* plants showed an enhanced apical dominance and only started to develop secondary stems around 7 to 8 weeks after germination (n = 7). In addition, changes in axillary branching were observed (Figures 6B-G). Siliques that are fused at the petiole (Figure 6B) or clustered siliques at the same axil of a bract (Figure 6C) were observed. In some *RPS5Apro>>BTB* lines, secondary inflorescence meristems terminated precociously resulting in clustered siliques at the tip of the stem (Figures 6D and 6G). Single siliques were also observed at an axil of a cauline leaf (Figure 6G), and in several cases, both siliques and axillary stems (paraclades) developed from an axil (Figures 6E-F). These observations indicate that the internodes, stem portions between two siliques or leaves, were missing or reduced, and that this defect appears to be random along the stem axis since normal-sized internodes were often visible.

Overexpression of *BT1* alone, either driven by the *35S* or *RPS5A* promoters, did not result in similar phenotypes, suggesting that this is a dominant negative effect of meristem-specific expression of the BTB domain. Interestingly, in *RPS5Apro>>PID* plants and in plants overexpressing both *PID* and *BT1*, some of these internode and axillary branching defects were also observed (Figure 6G). This suggests that these phenotypes are not strictly related to the down-regulation of PID activity, but rather that internode size determination is dependent on the local balance between *PID* and *BT1* expression levels, and that the interaction between PID and BT1 plays an important role in internode patterning.

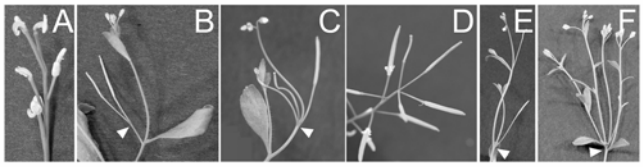

G

Phenotypes							n
PID-21 BT1-1	0.4/pl			0.5/pl	0.4/pl	0.6/pl	8
PID-21 BT1-2	1.5/pl			0.5/pl		1.3/pl	8
RPS5A>>BTB-1	2.9/pl	0.6/pl	0.6/pl	0.6/pl	0.3/pl	1.1/pl	8
RPS5A>>BTB-4	1.3/pl	0.4/pl	0.5/pl	0.5/pl			8
RPS5A>>BTB-5	1.3/pl		0.1/pl	0.1/pl		0.3/pl	8
RPS5A>>PID	0.6/pl						7
Col							9
PID-21							9
BT1-1					0.1/pl		8
BT1-2							8

Figure 6. *RPS5Apro>>BTB* expression results in axillary branch and inflorescence meristem defects.
(A-F) Phenotypes observed in *RPS5A>>BTB* plants. (A) Most of the plants develop primary inflorescence stems with few aberrant flowers that do not produce seeds. (B-F) Secondary inflorescences do develop fertile flowers and siliques that are occasionally fused at the petiole ((B), arrowhead), or clustered ((C), here three, arrowhead). Clustering of siliques is also observed at the inflorescence apex (D), probably due to early termination of the inflorescence meristem. Sometimes, single siliques can be found together with a paraclade at the axil of a cauline leaf ((E), arrowhead), or two paraclades are found at the same axil (F). Note that the next axil of a cauline leave also develops a paraclade, and that the internode length is strongly reduced.
(G) Table summarizing the frequencies of the different phenotypes (expressed as occurrence per plant) observed in the *RPS5Apro>>BTB* lines. Interestingly, some phenotypes are also observed in *35Spro:PID 35Spro:BT1* and *RPS5Apro>>PID* plants.

Discussion

An important characteristic of the plant hormone auxin is its polar transport which generates gradients and maxima that are instructive for cell division and growth during plant development. The chemiosmotic hypothesis proposed in the 1970's for the cell-to-cell transport of this hormone predicted that transporter proteins that drive the cellular efflux of auxin are themselves polarly localized (Rubery and Sheldrake, 1974, Raven, 1975). Later, the PIN proteins have been identified as auxin efflux carriers that determine the direction of transport through their asymmetric subcellular localization (Gälweiler et al., 1998, Wisniewska et al., 2006, Petrášek et al., 2006). In addition the protein kinase PID was found to control the direction of the auxin flux by regulating the subcellular localization of the PIN proteins (Friml et al., 2004). PID acts antagonistic to phosphatases through direct phosphorylation of PINs (Michniewicz et al., 2007). How this regulates the subcellular

targeting of PIN proteins, and which components are involved in the PID signaling pathway is largely unknown.

A yeast two-hybrid screen identified several PID interacting proteins, of which the two calcium binding proteins TCH3 and PBP1 have been described previously (Benjamins et al., 2003). Here we report the functional analysis of the plant specific BTB protein PINOID BINDING PROTEIN2 (PBP2), previously named BTB and TAZ domain protein1 (BT1). The interaction between PID and BT1/PBP2 was first identified in a yeast two-hybrid screen, and confirmed and confined to the BTB domain of BT1 by *in vitro* pull-down experiments. Northern blot analysis showed that the expression patterns of the two proteins overlap. Moreover, co-expression of CFP-tagged PID and YFP-tagged BT1 in Arabidopsis protoplasts resulted in recruitment of PID to the nucleus and BT1 to the plasma membrane, subcellular compartments where the single expressed proteins did not localize. This provided *in vivo* evidence for the interaction between PID and BT1.

BT1 as a negative regulator of PID kinase activity

For PBP1 and TCH3 it was demonstrated previously that they are not phospho-targets of PID, but that they bind PID to regulate its kinase activity in response to cytosolic calcium levels (Benjamins et al., 2003). Here we show that also BT1 is not phosphorylated by PID. Instead, BT1 reduced the activity of the kinase in *in vitro* phosphorylation assays, suggesting a role for BT1 as negative regulator of the PID pathway. This role was corroborated by the fact that *BT1* overexpression enhanced the *pid-14* loss-of-function embryo phenotypes and reduced the *PID* overexpression phenotypes. However, even though *BT1* overexpression reduced *PID* overexpression phenotypes, no striking and direct effect was observed on the PID-dependent basal to apical switch of PIN protein localization in *35Spro:PID-21 35Spro:BT1-1* roots. This result suggests that BT1 is not purely a negative regulator of PID activity, but that it rather modulates and fine tunes PID activity in different developmental processes.

This is corroborated by the observation that *BT1* overexpression does not affect *pid-14* inflorescences, whereas an enhancement of the pin-like phenotype is anticipated analogous to the enhanced cotyledon phenotypes of *pid-14 35Spro:BT1-1* embryos. The *35S* promoter is known to be active in floral meristems and in flowers (Bossinger and Smyth, 1996, Meister et al., 2005), and overexpression of other genes, e.g. MADS-box genes, using this promoter has lead to clear flower/inflorescence phenotypes (Robles and Pelaz, 2005). The absence of the effect of *BT1* overexpression on the *pid* inflorescence phenotype may be due to either (i) the non-availability of the BT1 scaffold protein for binding to other interactors in these tissues, (ii) a tissue specificity in the interaction between BT1 and PID and/or (iii) the increased instability of the BT1 protein in these tissues.

In Chapter 4 of this thesis we show that BT1 is an instable protein that is a target for degradation by the 26S proteasome, and that the instability is linked to the BTB domain. It would be interesting to test whether PID is part of this degradation process, and whether BT1 is involved in PID turn-over. The instability could explain why BT1 overexpression, both under control of the 35S or the meristem-specific *RPS5A* promoter (Weijers et al., 2001, Weijers et al., 2003) does not lead to clear phenotypic defects. However, meristem-specific overexpression of the BTB domain alone does provide clear dominant negative inflorescence phenotypes, which is expected if the BTB domain titrates out BT1 interactors such as PID to prevent their incorporation into their appropriate complexes.

Recently, a second BTB protein, the NPH3-like MACCHI BOU4/ENHANCER OF PINOID/NAKED PINS IN YUC MUTANTS1 (MAB4/ENP/NPY1), has been connected to the PID signaling pathway (Cheng et al., 2007, Furutani et al., 2007). The *mab4* loss-of-function mutation enhances *pid* phenotypes and affects PIN1 localization and expression in inflorescence meristem and embryo. MAB4 localizes in intracellular compartments, suggesting that MAB4, similar to BT1 is not a direct phospho-target of PID, but either a regulatory component of PID signaling or involved in a second parallel pathway that affects PIN polar targeting.

BT proteins as scaffold proteins in PINOID pathway

As predicted from its domain structure, BT1 is likely to serve as a scaffold protein that recruits PID to the appropriate signaling complex. PID interacts with the BTB domain of BT1, which in turn interacts with several other proteins, such as cytoskeleton related proteins or MYB domain proteins, through its TAZ domain (Kemel Zago, 2006). Analysis of the *35Spro:PID-21 bt1 bt2/+ bt3/ bt4 bt5* mutant indicates that the (nearly) absence of the BT function rescued the agravitropic growth and root meristem collapse observed in the *35Spro:PID-21* seedlings. This indicates that BT proteins are not merely negative regulators, but that they are important components of the PID signaling pathway. The inhibitory effect of BT1 on PID activity observed in *in vitro* phosphorylation assays and by overexpressing *BT1* in *pid-14* and *35Spro:PID-21* background may be the effect of BT1 blocking the PID catalytic domain during binding. In order to validate this conclusion, it would be interesting to investigate whether the apicalized PIN localization in is restored in the *bt* quintuple mutant. Moreover, besides rescue of the *PID* overexpression seedlings phenotypes, the *bt* quintuple mutant enhances phenotypes at the adult plant stage. Flowering *35Spro:PID-21* plants do not show clear phenotypes, whereas *35Spro:PID-21* quintuple *bt* mutant plants are bushy and develop short siliques, even shorter than observed in the quintuple *bt* mutant. This indicates that the effect of *PID* overexpression in the wild type background is masked by the BT proteins.

PID and BT1, a possible feed back loop between auxin and KNOX proteins

Interestingly, expressing the PID binding BTB domain under the *RPS5A* promoter leads to precocious arrest of the inflorescence meristem, production of infertile flowers, reduced internode elongation and apical dominance- and axillary branching defects. The fact that such phenotypes were not observed by overexpressing *BT1*, suggests that overexpression of the BTB domain has a dominant negative effect due to absence of the TAZ domain. However, some, but not all, of the axillary branching defects were also observed in the *RPS5Apro>>PID* and *35Spro:PID 35Spro:BT1* lines, indicating that these inflorescence phenotypes are not only caused by a reduction of PID activity. Based on the current data we hypothesize that rather an imbalance in the availability of PID and BT1 to interact, either by overexpressing one, both or a partial component, leads to subtle defects in the polar auxin transport. Correct localization of the PIN proteins at the SAM is crucial for a correct positioning of the auxin maxima that in turn controls the initiation and out growth of lateral organs, such as leaves and flowers (Reinhardt et al., 2003). Perturbing the correct activity of PID in these tissues affects the downstream PID-dependent processes and the siliques phyllotaxis.

Remarkably, clustered siliques are specific for the *RPS5Apro>>BTB* lines. Similar phenotypes are observed in loss-of-function mutants of the *BEL1-like homeobox* (*BEL*) gene *PENNYWISE* (*PNY*) (Smith and Hake, 2003). PENNYWISE and its orthologous protein POUND-FOOLISH (PNF) interact with the Knotted1-like homeobox (KNOX) proteins BREVIPEDICELLUS (BP) and SHOOTMERISTEMLESS (STM) (Kanrar et al., 2006). These BEL-KNOX heterodimers are responsible for internode patterning. Interestingly, BP and a microtubule-associated protein MPB2C (Kragler et al., 2003) were found to interact with BT1 in the yeast two-hybrid system (Kemel Zago, 2006)). Recently, MPB2C was found to interact with STM to prevent its cell-to-cell transport (Winter et al., 2007). At the same time, auxin and the PIN transporter protein-mediated polar distribution of this hormone control inflorescence architecture, by regulating apical dominance, internode elongation and phyllotaxis (Reinhardt et al., 2003, Leyser, 2003, Woodward et al., 2005). A recent paper identified the LOB domain protein JAGGED LATERAL ORGANS (JLO) as activator of BP expression and repressor of PIN expression (Borghi et al., 2007). Loss-of-function *bp* partially rescues *pid* and *pin1* flower phenotype, and correct auxin transport regulation is necessary to promote leaf development by repressing *BP* expression (Hay et al., 2006). Moreover, the maize *rough sheat2* mutant that overexpresses three *KNOX* genes shows decreased polar auxin transport (Tsiantis et al., 1999). Clearly there is a complex network of interactions between auxin transport and signaling and the action of KNOX and BEL proteins. The BT1 scaffold protein could be part of a feed back loop through its interaction with PID, MPB2C and BP.

Material and Methods

Yeast two-hybrid screen, molecular cloning and constructs

The yeast two-hybrid screen has been described previously (Benjamins et al., 2003). Molecular cloning was performed following standard procedures (Sambrook et al., 1989). The complete coding region of *PID*, excluding the start codon, was amplified using primers PID-*Sal*I-F1 (5'GG-*Sal*I-TTACGAGAATCAGACGGTGAG3') and PID-*Xba*I-R1 (5'CC-*Xba*I-CCGTAGAAAACGTTCAAAAGT3') and cloned into pBluescriptSK+ to create pSDM6005. The cDNA of *PID* was then N-terminally fused (*Xmn*I-*Sal*I) to the His-tag (10x His) present in pET16H (Klenow blunted *BamH*I-*Xho*I), a derivative of pET16B (J. Memelink, unpublished results). The construct pSDM6004 (pGEX-PID) has been described elsewhere (Benjamins et al., 2003). The *35Spro:PID:GFP* construct was generated by amplifying the *PID* cDNA using the primers 5'TTAATATGACTCACTATAGG3' and 5'GCTCACCATAAAGTAATCGAACGC3' and the *eGFP* coding region using the primers 5'GATTACTTTATGGTGAGCAAGGGC3' and 5'TCAATCTGAGTACTTGTACAG3'. Both PCR products were used in a fusion PCR with outer primers, and the amplified *PID:GFP* fragment was cloned into pUC28 digested with *Nco*I and *Hin*cII, and excised again with *Eco*RI and *Stu*I (blunted) for ligation into *Eco*RI-*Sma*I digested pART7. The *35Spro:PID:CFP* construct was made using the Gateway Technology (Invitrogen). *PID* cDNA was PCR amplified from pSDM6004 (pGEX:PID) (Benjamins et al., 2003) with primers containing *att*B recombination sites (underlined):
5'GGGGACAAGTTTGTACAAAAAAGCAGGCTTCAGCATGTTACGAGAATCAGAC GGT3' and
5'GGGGACCACTTTGTACAAGAAAGCTGGGTCAAAGTAATCGAACGCCGCTGG3' BP reaction was performed in pDONOR207 according to manufacturer's instructions (Invitrogen). Recombinant plasmid was isolated and sequenced. LR reaction was performed in pART7 plasmids containing the CFP fluorescent markers in frame with the gateway recombinant cassette (C. Galvan-Ampudia, unpublished data).

The plasmids pSDM6014 (pBS-BT1), pSDM6069 (pUC28-BT2), pSDM6086 (pC1300-BT1), pSDM6092 (pUC28-BT4), pSDM6099 (pART7-BT1:YFP) and pDM6309 (pDONOR207-BT3) were previously described (Chapter 4, this thesis). The cDNA of *BT1* (*Xho*I-*Sma*I digested from pSDM6014), excluding the start codon, was cloned into pGEX-KG (Guan and Dixon, 1991) to obtain pGEX-BT1 encoding an N-terminal GST-BT1 fusion. The plasmid pGEX-BTB, encoding the GST-tagged BT1 BTB/POZ domain, was generated by digesting pGEX-BT1 with *Nde*I and filling in with Klenow. The plasmid pGEX-TAZ, encoding the GST-tagged BT1 TAZ domain, was constructed by deleting the *Nco*I fragment from pGEX-BT1. For the N-terminal His-BT1 fusion used within the *in vitro* pull-down and the *in vitro* phosphorylation assay experiments, the *BT1* coding region

which excluded the start codon was cloned as a *Xho*I-*Sma*I fragment into pET16H (pSDM6006).The *BT2* cDNA was cloned (*Eco*RI-*Bam*HI from pSDM6069) in frame with a His-tag in pET16H (pSDM6078). The *BT4* cDNA was cloned (*Eco*RI-*Bam*HI from pSDM6092) in frame with the His-tag in pET16H (pSDM6093). The translational fusion between *BT5* cDNA (from pSDM6309) and the His-tag was generated into the pET16H derived destination vector (pSDM6310) (C. Galvan-Ampudia, unpublished data) using the Gateway technology (Invitrogen). To construct pEF-BT1, *BT1* cDNA was cloned as an *Eco*RI-*Kpn*I fragment from pSUMFUNdelta*Nco*I-BT1s (Y. Xiong, unpublished data) into pIC-UAS-E-tNOS, derived from pSDM7022 (Weijers et al., 2003). To construct pEF-BTB, the *Nco*I fragment containing the BTB part of BT1 from pGEX-BT1 was cloned into pUC28. The BTB domain (*Bam*HI-*Eco*RI) was then fused to the UAS promoter into pIC-UAS-E-tNOS. The expression cassettes *UAS-E-BT1-tNOS* and *UAS-E-BTB-tNOS* were then transferred as a *Hin*dIII fragment from pIC-UAS-E-BT1-tNOS or pIC-UAS-E-BTB-tNOS respectively into pSDM7006 (Weijers et al., 2003).

***Arabidopsis* lines, plant growth, transformation and protoplast transfections**

The *35Spro:PID*-21 line (Benjamins et al., 2001), the *PIDpro:PID:VENUS* line (Michniewicz et al., 2007), the quintuple mutant *bt1 bt2/+ bt3/+ bt4 bt5* (Chapter 4, this thesis) and *pid-14* allele (SALK_049736) (Chapter 2, this thesis) were described previously.

Arabidopsis seeds were surfaced-sterilized by incubation for 15 min in 50 % commercial bleach solution and rinsed four times with sterile water. Seeds were vernalized for 2 to 4 days before germination (21^{o}C, 16-hour photoperiod and 3000 lux) on solid MA medium (Masson and Paszkowski, 1992) supplemented with antibiotics when required. Two- to three-week old plants were transferred to soil and grown at 21^{o}C with a 16-hour photoperiod of 10000 lux and at 70 % relative humidity.

Arabidopsis thaliana ecotype Columbia (Col) was transformed by floral dipping method as described (Clough and Bent, 1998) using *Agrobacterium tumefaciens* strain LBA1115. The binary construct *35Spro:BT1* was transformed into *Arabidopsis* Col plants. The constructs *EF-BT1* and *EF-BTB* were transformed into the *ACT-RPS5A*-5 line (Weijers et al., 2003). Primary transformants were selected on medium supplemented with 20 µg/ml hygromycin for the *35S* constructs or 30 µg/ml phosphinotricin and 25 µg/ml kanamycin for the *EF* constructs and 100 µg/ml timentin to inhibit *Agrobacterium* growth. For further analysis, single locus insertion lines were selected by segregation on hygromycin at 10 µg/ml or phosphinotricin at 15 µg/ml and analyzed for expression by Northern blot analysis (*35Spro:BT1*).

Protoplasts were obtained from Arabidopsis Col cell suspension cultures that were propagated as described (Schirawski et al., 2000). Protoplast isolation and PEG-mediated transfections were performed as initially described (Axelos et al., 1992) and adapted by

Schirawski and coworkers (Schirawski et al., 2000). Transfections were performed with 20 µg (*35Spro:GFP*, *35Spro:PID:GFP*) or 5 µg (*35Spro:PID:CFP*, *35Spro:BT1:YFP*) of plasmid DNA, after which the cells were incubated for at least 16 h prior observation using confocal laser scanning microscopy.

***In vitro* pull down experiments**

E. coli strain Rosetta (Novagen) was transformed with pGEX, pSDM6004, pSDM6006, pSDM6078, pSDM6093 and pSDM6310. And His-tagged PID and GST-tagged BT1, BTB/POZ and TAZ or GST alone were expressed and purified from *E. coli* strain BL21-DE03. *E. coli* cells containing one of the constructs were grown at 37°C to OD_{600} 0.8 in 50 ml LC supplemented with antibiotics. The cultures were then induced for 4 h with 1 mM IPTG at 30°C, after which cells were harvested by centrifugation (10 min, 4000 rpm) and stored at -20°C. Precipitated cells were resuspended in 2 ml Extraction Buffer (EB: 1x PBS, 2 mM EDTA, 2 mM DTT) supplemented with 0.1 mM PMSF (Phenylmethanesulfonyl Fluoride), 0.1 mM Leupeptin and 0.1 mM Aprotinin for the GST-tagged proteins or in 2 ml Binding Buffer (50 mM Tris-HCl pH 6.8, 100 mM NaCl, 10 mM $CaCl_2$) supplemented with 0.1 mM PMSF, 0.1 mM Leupeptin and 0.1 mM Aprotinin for His-tagged proteins and sonicated for 2 min on ice. From this point on, all steps were performed at 4°C. Eppendorf tubes containing the sonicated cells were centrifuged at 14000 rpm for 20 min. The supernatant containing His-tagged proteins was left on ice, while 100 µl Glutathione Sepharose 4B resin (Amersham-Pharmacia) (pre-equilibrated with three washes of 10 resin volumes of 1x PBS followed by three washes of 10 resin volumes of 1x EB at 500 g for 5 min) was added to the GST-fusion proteins containing supernatants. Resin-containing mixtures were incubated for 1 h with gentle agitation, subsequently centrifuged at 500 g for 3 min and the precipitated resin was washed three times with 20 resin volumes of EB. Next, His-tagged proteins containing supernatant (approximately 2 ml) was added to GST-fusions-containing resins, and the mixtures were incubated for 1 h with gentle agitation. After incubation, supernatants containing GST resins were centrifuged at 500 g for 3 min, the new supernatants were discarded and the resins subsequently washed three times with 20 resin volumes of EB. Protein loading buffer was added to the resin samples, followed by denaturation for 5 min at 95°C. Proteins were subsequently separated on a 10 % (BT proteins pull-down assay) or 12 % (Domains pull-down assay) polyacrylamide gel prior to transfer to an Immobilon-P PVDF (Millipore) membrane. Western blots were hybridized using a horse radish peroxidase (HRP)-conjugated anti-penta Histidine antibody (Qiagen) and detection followed the protocol described for the Phototope-HRP Western Blot Detection Kit (New England Biolabs). A parallel gel was run and stained with Coomassie as loading control.

***In vitro* phosphorylation assays**

His-tagged proteins were purified from 5 aliquots of 50 ml cultures of *E. coli*. BL21 cells which were grown, induced, pelleted and frozen as described above for the *in vitro* pull down experiments. Commercial Myelin Basic Protein (MBP, Sigma) was used a positive control. Each aliquot of frozen cell pellet was resuspended in 2 ml Lysis Buffer (LB: 25 mM Tris-HCl pH 8.0, 500 mM NaCl, 20 mM Imidazol, 0.1 % Tween-20) supplemented with 0.1 mM PMSF, 0.1 mM Leupeptin and 0.1 mM Aprotinin and sonicated for 2 min on ice. Further steps were performed at 4^{o}C. Sonicated cells were centrifuged at 14000 rpm for 20 min, supernatants from all aliquots of the same construct were transferred to a 15 ml tube containing 100 µl of pre-equilibrated Ni-NTA resin (Qiagen) (pre-equilibration performed with three washes of 10 resin volumes of LB at 500 g for 5 min). Supernatant and resin were mixed, incubated with gentle agitation for 1 h, after which the resin was collected by centrifugation at 500 g for 3 min. The resin was washed three times with 20 resin volumes of LB, once with 20 resin volumes of Wash Buffer 1 (25 mM Tris-HCl pH 8.0, 500 mM NaCl, 40 mM Imidazol, 0.05 % Tween-20) and once with 20 resin volumes of Wash Buffer 2 (25 mM Tris-HCl pH 8.0, 600 mM NaCl, 80 mM Imidazol). After the last washing step, the resin was incubated in 20 volumes of Elution Buffer (25 mM Tris-HCl pH 8.0, 500 mM NaCl, 500 mM Imidazol) for 15 min with gentle agitation. The resin was centrifuged for 3 min at 500 g, and the supernatant containing the desired protein was diluted a 1000-fold in Tris Buffer (25 mM Tris-HCl pH 7.5, 1 mM DTT) and concentrated to a workable volume (usually 50 µl) using Vivaspin microconcentrators (10 kDa cut off, maximum capacity 600 µl, Vivascience). Glycerol was added as preservative to 10 % final concentration and samples were stored at -80^{o}C.

Approximately 1 µg of purified His-tag protein (PID and substrate) was added to a 20 µl kinase reaction mix, containing 1x kinase buffer (25 mM Tris-HCl pH 7.5, 1 mM DTT, 5 mM $MgCl_2$) and 1 x ATP solution (100 µM $MgCl_2$, 100 µM ATP-Na_2, 1 µCi ^{32}P-γ-ATP). Reactions were incubated at 30^{o}C for 30 min and stopped by addition of 5 µl of 5x protein loading buffer (310 mM Tris-HCl pH 6.8, 10 % SDS, 50 % Glycerol, 750 mM β-Mercaptoethanol, 0.125 % Bromophenol Blue) and 5 min boiling. Reactions were subsequently separated over 12.5 % acrylamide gels, which were washed three times for 30 min with Kinase Gel Wash Buffer (5 % Trichoroacetic Acid, 1 % $Na_2H_2P_2O_7$), Coomassie stained and dried. Autoradiography was performed for 24 to 48 h at -80^{o}C using Fuji Super RX X-ray films and intensifier screens.

RNA extraction and Northern Blots

Total RNA was purified using the RNeasy Plant Mini kit (Qiagen). Subsequent RNA blot analysis was performed as described (Memelink et al., 1994) using 10 µg of total RNA per sample. The following modifications were made: pre-hybridizations and hybridizations were conducted at 65^{o}C using a different hybridization mix (10 % Dextran sulfate, 1 %

SDS, 1 M NaCl, 50 µg/ml of single strand Herring sperm DNA). The hybridized blots were washed for 20 min at 65°C in 2x SSPE 0.5 % SDS, and for 20 min at 42°C in respectively 0.2x SSPE 0.5 % SDS, 0.1x SSPE 0.5 % SDS and 0.1x SSPE. Blots were exposed to X-ray film FUJI Super RX. Probes were PCR amplified and column purified (Qiagen): 5'CATCCCAAACATTACAAAGGGC3', 5'TTCTCCGAGGTTCGTCTTTC3' for *BT1* from pSDM6006; 5'AGGCACGTGACAACGTCTC3', 5'CGCAAGACTCGTTGGAAAAG3' for *PID* from Col genomic DNA; 5'CGGAATTCATGAGAGAGATCCTTCATATC3', 5'CCCTCGAGTTAAGTCTCGTACTCCTCTTC3' for *αTubulin* from Col genomic DNA; 5'CGGGAAGGATCGTGATGGA3', 5'CCAACCTTCTCGATGGCCT3' for *AtROC* from Col genomic DNA. Probes were radioactively labeled using α-^{32}P-ATP (Amerscham) and a Prime-a-gene kit (Promega).

Immunolocalization

Whole-mount immunolocalizations were performed on 3-day old seedlings fixed in 4 % paraformaldehyde in MTSB buffer as described previously (Friml et al., 2003) using medium size baskets format in an InSituPro robot (INTAVIS, Cologne, Germany). Rabbit anti-PIN1 and anti-PIN2 primary antibodies (1/400) and Alexa 488-conjugated anti-rabbit secondary antibodies (1/200, Molecular Probes) were used for detection. Samples were observed using confocal laser scanning microscopy.

Biological assays

For the root meristem collapse assay, about 200 seedlings per line were grown in triplicate on vertical plates on MA medium, while the development of the seedling root was monitored and scored each day during eight days for the collapse of the primary root meristem. For the phenotypic analysis of *35Spro:BT1 pid-14/+* lines, about 300 seeds (200 for *35Spro:BT1-1*) were plated in triplicate on MA medium and germinated for one week. The number of dicotyledon seedlings and of seedlings with specific cotyledon defects was counted and the penetrance of the specific phenotypes was calculated based on a 1:3 segregation ratio for *pid/pid* seedlings. To test for auxin responsive gene expression, one-week old Arabidopsis Col seedlings were transferred to liquid MA medium under shaking conditions. After 3 days of culture, seedlings were treated with 5 µM IAA for the indicated time.

Confocal Laser Scanning Microscopy

YFP fusion lines and immunolocalizations were observed using 40x dry and oil objectives on a ZEISS Axioplan microscope equipped with a confocal laser scanning unit (MRC1024ES, BIO-RAD, Hercules, CA). The YFP and Alexa 488 fluorescences were monitored with a 522-532 nm band pass emission filter (488 nm excitation). All images

were recorded using a 3CCD Sony DKC5000 digital camera. For the protoplast experiments, a Leica DM IRBE confocal laser scanning microscope was used with a 63x water objective. The fluorescence was visualized with an Argon laser for excitation at 488 nm (GFP), 514 nm (YFP) and 457 nm (CFP) with 522-532 nm (GFP), 527-560 nm (YFP) and 467-499 nm (CFP) emission filters. The images were processed by ImageJ (http://rsb.info.nih.gov/ij/) and assembled in Adobe Photoshop 7.0.

Accession Numbers

The Arabidopsis Genome Initiative locus identifiers for the genes mentioned in this article are as follows: *BT1/PBP2* (At5g63160), *BT2/PBP2H1* (At3g48360), *BT3/PBP2H2* (At1g05690), *BT4/PBP2H4* (At5g67480), *BT5/PBP2H3* (At4g37610), *PID* (At2g34650), *PIN1* (At1g73590), *PIN2* (At5g57090), *TCH3* (At2g41100), *PBP1* (At5g54490), *ROC* (At4g38740), *αTubulin* (At5g44340), *PNY* (At5g02030), *PNF* (At2g27990), *BP* (At4g08150), *STM* (At1g62230), *JLO* (At4g00220), *NPH3* (At5g64330), *RPT2* (At2g30520), *CUL3a* and *b* (At1g26830 and At1g69670), *MAB4/ENP* (At4g31820), *BET10/GTE11* (At3g01770), *BET9/GTE* (At5g14270) and *TAC1* (At3g09290).

Acknowledgements

We would like to thank Ward Winter for their technical assistance, Gerda Lamers for her helpful advises concerning microscopy, Jiří Friml and Christian Luschnig for providing respectively PIN1 and PIN2 antibodies, M. Heilser for the *PIDpro:PID:VENUS* seeds and Pieter Ouwerkerk for kindly providing the pCambia1300int-35Snos and pCAMBIA1300 plasmids. This work was financially supported by the Brazilian Funding Agency for Post-Graduation Education-CAPES (M.K.Z.), and by Earth and Life Sciences (ALW) with financial support from the Dutch Organization of Scientific Research (NWO, C. G-A.).

References

Albagli,O., Dhordain,P., Deweindt,C., Lecocq,G., and Leprince,D. (1995). The BTB/POZ domain: a new protein-protein interaction motif common to DNA- and actin-binding proteins. Cell Growth Differ **6**:1193-1198.

Axelos,M., Curie,C., Mazzolini,L., Bardet,C., and Lescure,B. (1992). A Protocol for Transient Gene-Expression in Arabidopsis-Thaliana Protoplasts Isolated from Cell-Suspension Cultures. Plant Physiology and Biochemistry **30**:123-128.

Bardwell,V.J. and Treisman,R. (1994). The Poz Domain - A Conserved Protein-Protein Interaction Motif. Genes & Development **8**:1664-1677.

Benjamins, R. (2004). Functional analysis of the PINOID protein kinase in *Arabidopsis thaliana*. Institute of Biology, Leiden University, The Netherlands.

Benjamins,R., Galván-Ampudia,C.S., Hooykaas,P.J., and Offringa,R. (2003). PINOID-mediated signaling involves calcium-binding proteins. Plant Physiol **132**:1623-1630.

Benjamins,R., Quint,A., Weijers,D., Hooykaas,P., and Offringa,R. (2001). The PINOID protein kinase regulates organ development in Arabidopsis by enhancing polar auxin transport. Development **128**:4057-4067.

Benková,E., Michniewicz,M., Sauer,M., Teichmann,T., Seifertová,D., Jürgens,G., and Friml,J. (2003). Local, efflux-dependent auxin gradients as a common module for plant organ formation. Cell **115**:591-602.

Bennett,S.R.M., Alvarez,J., Bossinger,G., and Smyth,D.R. (1995). Morphogenesis in Pinoid Mutants of Arabidopsis-Thaliana. Plant J. **8**:505-520.

Borghi,L., Bureau,M., and Simon,R. (2007). Arabidopsis JAGGED LATERAL ORGANS Is Expressed in Boundaries and Coordinates KNOX and PIN Activity. Plant Cell:1795-1808.

Bossinger,G. and Smyth,D.R. (1996). Initiation patterns of flower and floral organ development in Arabidopsis thaliana. Development **122**:1093-1102.

Cheng,Y., Qin,G., Dai,X., and Zhao,Y. (2007). NPY1, a BTB-NPH3-like protein, plays a critical role in auxin-regulated organogenesis in Arabidopsis. Proc.Natl.Acad.Sci.U.S.A.

Christensen,S.K., Dagenais,N., Chory,J., and Weigel,D. (2000). Regulation of auxin response by the protein kinase PINOID. Cell **100**:469-478.

Clough,S.J. and Bent,A.F. (1998). Floral dip: a simplified method forAgrobacterium-mediated transformation ofArabidopsis thaliana. Plant J. **16**:735-743.

Dieterle,M., Thomann,A., Renou,J.P., Parmentier,Y., Cognat,V., Lemonnier,G., Muller,R., Shen,W.H., Kretsch,T., and Genschik,P. (2005). Molecular and functional characterization of Arabidopsis Cullin 3A. Plant J. **41**:386-399.

Du,L.Q. and Poovaiah,B.W. (2004). A novel family of Ca2+/calmodulin-binding proteins involved in transcriptional regulation: interaction with fsh/Ring3 class transcription activators. Plant Molecular Biology **54**:549-569.

Figueroa,P., Gusmaroli,G., Serino,G., Habashi,J., Ma,L.G., Shen,Y.P., Feng,S.H., Bostick,M., Callis,J., Hellmann,H., and Deng,X.W. (2005). Arabidopsis has two redundant Cullin3 proteins that are essential for embryo development and that interact with RBX1 and BTB proteins to form multisubunit E3 ubiquitin ligase complexes in vivo. Plant J. **17**:1180-1195.

Friml,J., Benková,E., Mayer,U., Palme,K., and Muster,G. (2003). Automated whole mount localisation techniques for plant seedlings. Plant J. **34**:115-124.

Friml,J., Yang,X., Michniewicz,M., Weijers,D., Quint,A., Tietz,O., Benjamins,R., Ouwerkerk,P.B.F., Ljung,K., Sandberg,G., Hooykaas,P.J.J., Palme,K., and Offringa,R. (2004). A PINOID-dependent binary switch in apical-basal PIN polar targeting directs auxin efflux. Science **306**:862-865.

Furutani,M., Kajiwara,T., Kato,T., Treml,B.S., Stockum,C., Torres-Ruiz,R.A., and Tasaka,M. (2007). The gene MACCHI-BOU 4/ENHANCER OF PINOID encodes a NPH3-like protein and reveals similarities between organogenesis and phototropism at the molecular level. Development.

Gälweiler,L., Guan,C., Müller,A., Wisman,E., Mendgen,K., Yephremov,A., and Palme,K. (1998). Regulation of polar auxin transport by AtPIN1 in Arabidopsis vascular tissue. Science **282**:2226-2230.

Gingerich,D.J., Gagne,J.M., Salter,D.W., Hellmann,H., Estelle,M., Ma,L.G., and Vierstra,R.D. (2005). Cullins 3a and 3b assemble with members of the broad complex/tramtrack/bric-a-brac (BTB) protein family to form essential ubiquitin-protein ligases (E3s) in Arabidopsis. J.Biol.Chem. **280**:18810-18821.

Guan,K.L. and Dixon,J.E. (1991). Eukaryotic Proteins Expressed in Escherichia-Coli - An Improved Thrombin Cleavage and Purification Procedure of Fusion Proteins with Glutathione-S-Transferase. Analytical Biochemistry **192**:262-267.

Hay,A., Barkoulas,M., and Tsiantis,M. (2006). ASYMMETRIC LEAVES1 and auxin activities converge to repress BREVIPEDICELLUS expression and promote leaf development in Arabidopsis. Development **133**:3955-3961.

Kanrar,S., Onguka,O., and Smith,H. (2006). Arabidopsis inflorescence architecture requires the activities of KNOX-BELL homeodomain heterodimers. Planta **224**:1163-1173.

Kemel Zago, M. (2006). Components and targets of the PINOID signaling complex in *Arabidopsis thaliana*. Institute of Biology, Leiden University, The Netherlands.

Kragler,F., Curin,M., Trutnyeva,K., Gansch,A., and Waigmann,E. (2003). MPB2C, a microtubule-associated plant protein binds to and interferes with cell-to-cell transport of tobacco mosaic virus movement protein. Plant Physiol **132**:1870-1883.

Lee,S.H. and Cho,H.T. (2006). PINOID positively regulates auxin efflux in Arabidopsis root hair cells and tobacco cells. Plant Cell **18**:1604-1616.

Leyser,O. (2003). Regulation of shoot branching by auxin. Trends Plant Sci. **8**:541-545.

Masson,J. and Paszkowski,J. (1992). The Culture Response of Arabidopsis-Thaliana Protoplasts Is Determined by the Growth-Conditions of Donor Plants. Plant J. **2**:829-833.

Meister,R.J., Oldenhof,H., Bowman,J.L., and Gasser,C.S. (2005). Multiple Protein Regions Contribute to Differential Activities of YABBY Proteins inReproductive Development. Plant Physiol. **137**:651-662.

Memelink,J., Swords,K.M.M., Staehelin,L.A., and Hoge,J.H.C. (1994) Southern, Northern and Western blot analysis. In Plant Molecular Biology Manuel, (Dordrecht, NL: Kluwer Academic Publishers).

Michniewicz,M., Zago,M.K., Abas,L., Weijers,D., Schweighofer,A., Meskiene,I., Heisler,M.G., Ohno,C., Huang,F., Weigel,D., Meyerowitz,E.M., Luschnig,C., Offringa,R., and Friml,J. (2007). Antagonistic regulation of PIN phosphorylation by PP2A and PINOID directs auxin flux. Cell **130**:1044-1056.

Motchoulski,A. and Liscum,E. (1999). Arabidopsis NPH3: A NPH1 photoreceptor-interacting protein essential for phototropism. Science **286**:961-964.

Okada,K., Ueda,J., Komaki,M.K., Bell,C.J., and Shimura,Y. (1991). Requirement of the Auxin Polar Transport System in Early Stages of Arabidopsis Floral Bud Formation. Plant Cell **3**:677-684.

Paponov,I.A., Teale,W.D., Trebar,M., Blilou,I., and Palme,K. (2005). The PIN auxin efflux facilitators: evolutionary and functional perspectives. Trends Plant Sci. **10**:170-177.

Petrášek,J., Mravec,J., Bouchard,R., Blakeslee,J.J., Abas,M., Seifertová,D., Wisniewska,J., Tadele,Z., Kubes,M., Covanová,M., Dhonukshe,P., Skupa,P., Benková,E., Perry,L., Krecek,P., Lee,O.R., Fink,G.R., Geisler,M., Murphy,A.S., Luschnig,C., Zazimalová,E., and Friml,J. (2006). PIN Proteins Perform a Rate-Limiting Function in Cellular Auxin Efflux. Science **312**:914-918.

Ponting,C.P., Blake,D.J., Davies,K.E., Kendrick-Jones,J., and Winder,S.J. (1996). ZZ and TAZ: new putative zinc fingers in dystrophin and other proteins. Trends in Biochemical Sciences **21**:11-13.

Raven,J.A. (1975). Transport of indolaceticacid in plant cells in relation to pH and electrical potential gradients, and its significance for polar IAA transport. New Phytologist **74**:163-172.

Reinhardt,D., Pesce,E.R., Stieger,P., Mandel,T., Baltensperger,K., Bennett,M., Traas,J., Friml,J., and Kuhlemeier,C. (2003). Regulation of phyllotaxis by polar auxin transport. Nature **426**:255-260.

Robles,P. and Pelaz,S. (2005). Flower and fruit development in Arabidopsis thaliana. Int.J.Dev.Biol. **49**:633-643.

Rubery,P.H. and Sheldrake,A.R. (1974). Carrier-mediated auxin transport. Planta **118**:101-121.

Sabatini,S., Beis,D., Wolkenfelt,H., Murfett,J., Guilfoyle,T., Malamy,J., Benfey,P., Leyser,O., Bechtold,N., Weisbeek,P., and Scheres,B. (1999). An auxin-dependent distal organizer of pattern and polarity in the Arabidopsis root. Cell **99**:463-472.

Sakai,T., Wada,T., Ishiguro,S., and Okada,K. (2000). RPT2. A signal transducer of the phototropic response in Arabidopsis. Plant Cell **12**:225-236.

Sambrook,J., Fritsch F., and Maniatis,T. (1989) Molecular cloning - A laboratory Manual. New York: Cold Spring Harbor Laboratory press, ed.

Schirawski,J., Planchais,S., and Haenni,A.L. (2000). An improved protocol for the preparation of protoplasts from an established Arabidopsis thaliana cell suspension culture and infection with RNA of turnip yellow mosaic tymovirus: a simple and reliable method. Journal of Virological Methods **86**:85-94.

Smith,H.M.S. and Hake,S. (2003). The Interaction of Two Homeobox Genes, BREVIPEDICELLUS and PENNYWISE, Regulates Internode Patterning in the Arabidopsis Inflorescence. Plant Cell **15**:1717-1727.

Tanaka,H., Dhonukshe,P., Brewer,P.B., and Friml,J. (2006). Spatiotemporal asymmetric auxin distribution: a means to coordinate plant development. Cell Mol.Life Sci. **63**:2738-2754.

Tsiantis,M., Brown,M.I.N., Skibinski,G., and Langdale,J.A. (1999). Disruption of Auxin Transport Is Associated with Aberrant Leaf Development in Maize. Plant Physiol. **121**:1163-1168.

Wang,K.L.C., Yoshida,H., Lurin,C., and Ecker,J.R. (2004). Regulation of ethylene gas biosynthesis by the Arabidopsis ETO1 protein. Nature **428**:945-950.

Weber,H., Bernhardt,A., Dieterle,M., Han,P., Hano,P., Mutlu,A., Estelle,M., Genschik,P., and Hellmann,H. (2005). Arabidopsis AtCUL3a and AtCUL3b form complexes with members of the BTB/POZ-MATH protein family. Plant Physiol. **137**:83-93.

Weijers,D., Franke-van Dijk,M., Vencken,R.J., Quint,A., Hooykaas,P., and Offringa,R. (2001). An Arabidopsis Minute-like phenotype caused by a semi-dominant mutation in a RIBOSOMAL PROTEIN S5 gene. Development **128**:4289-4299.

Weijers,D., van Hamburg,J.P., van Rijn,E., Hooykaas,P.J.J., and Offringa,R. (2003). Diphtheria Toxin-Mediated Cell Ablation Reveals Interregional Communication during Arabidopsis Seed Development. Plant Physiol. **133**:1882-1892.

Winter,N., Kollwig,G., Zhang,S., and Kragler,F. (2007). MPB2C, a microtubule-associated protein, regulates non-cell-autonomy of the homeodomain protein KNOTTED1. Plant Cell **19**:3001-3018.

Wisniewska,J., Xu,J., Seifertová,D., Brewer,P.B., Ruzicka,K., Blilou,I., Rouquié,D., Benková,E., Scheres,B., and Friml,J. (2006). Polar PIN localization directs auxin flow in plants. Science **312**:883.

Woodward,C., Bemis,S.M., Hill,E.J., Sawa,S., Koshiba,T., and Torii,K.U. (2005). Interaction of auxin and ERECTA in elaborating Arabidopsis inflorescence architecture revealed by the activation tagging of a new member of the YUCCA family putative flavin monooxygenases. Plant Physiol **139**:192-203.

Zimmermann,P., Hirsch-Hoffmann,M., Hennig,L., and Gruissem,W. (2004). GENEVESTIGATOR. Arabidopsis microarray database and analysis toolbox. Plant Physiol. **136**:2621-2632.